PAPER • OPEN ACCESS

Low-power, fast-response active gas-gap heat switches for low temperature applications

To cite this article: Mark O Kimball *et al* 2015 *IOP Conf. Ser.: Mater. Sci. Eng.* **101** 012157

View the article online for updates and enhancements.

Low-power, fast-response active gas-gap heat switches for low temperature applications

Mark O Kimball[1], Peter J Shirron[1], Bryan L James[1], Theodore T Muench[1], Michael A Sampson[2] and Richard V Letmate[3]

[1]NASA Goddard Space Flight Center, 8800 Greenbelt Road, Greenbelt, MD 20771, U.S.A.
[2]SGT Inc., 7701 Greenbelt Road, Suite 400 Greenbelt, MD 20770, U.S.A
[3]Bastion Technologies, 7515 Mission Drive, Suite 300 Lanham, MD 20706, U.S.A

E-mail: `mark.o.kimball@nasa.gov, peter.j.shirron@nasa.gov`

Abstract. Heat switches are critical to many low temperature applications, where control of heat flow and selective thermal isolation are required. Their designs tend to be driven by the need for the lowest possible off-state conductance, while meeting requirements for on-state conduction. As a result, heat switches tend to be designed as close as possible to the limits of material strength and machinability, using materials that have the lowest thermal conductivity to strength ratio. In addition, switching speed is important for many applications, and many designs and switch types require a compromise between the power used for actuation and on/off transition times. We present a design for an active gas-gap heat switch, developed for the Soft X-ray Spectrometer instrument on the Japanese Astro-H mission, that requires less than 0.5 mW of power to operate, has on/off transition times of < 1 minute, and that achieves a conductance of > 50 mW/K at 1 K with a heat leak of < 0.5 μW from 1 K to very low temperature. Details of the design and performance will be presented.

1. Introduction

Heat switches, as the name implies, are devices that control the flow of heat in thermal systems. In the conductive state (on or closed) they allow heat to pass from one region in the system to another. In the insulating state (off or open) they isolate two regions.

Heat switches come in many forms and are typically named based upon the underlying mechanism for their switching behavior: gas-gap, superconducting, magneto-restrictive, mechanical, etc. For instance, in a mechanical heat switch, two conductors are brought together, typically with a high force, to allow heat to flow through the switch and taken apart to end the flow. In a superconducting heat switch, the temperature of a superconducting material may be lowered to allow the superconducting state to form which, in turn, initiates an energy gap in the continuum of energy states. This suppresses the number of unpaired electrons, the main carriers of thermal energy at low temperature in these materials.

Gas-gap heat switches, the focus of this paper, rely upon adding or removing gas from the interior of the switch body to link or unlink portions of the switch. Inside the hermetically sealed switch body are two conductors that are attached to one end or the other and separated from one another. When gas is evacuated from the body, there is no conduction between the interior conductors and, if the temperature is low enough, no radiative coupling as well. Therefore, if gas is removed from the switch interior, the two ends are connected only by the outer shell.

(a) Switch ready for integration
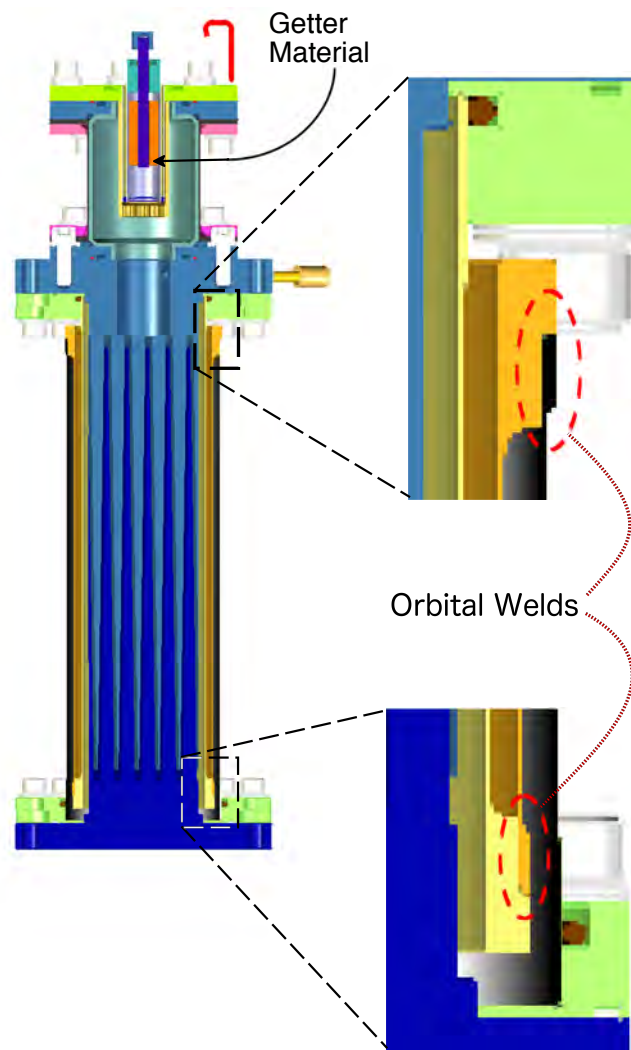
(b) Cut-away view of heat switch with enlarged views of the orbital-welded joints that allow the reentrant titanium shell; see text.

Figure 1. A complete heat switch ready to be integrated into the ADR used to cool the Astro-H soft X-ray spectrometer detector array. The heat switch shell, discussed in detail below, is the cylinder that runs the majority of the length. Inside this are the tapered copper fins that are connected to either end of the heat switch shell but are separate from one another by a gap of 0.36 mm. The getter material is bituminous charcoal and is found within the structure at the top of the switch.

Thus, in the off state at low temperature, the heat leak from one end of the switch to the other is dictated by the conductance of the shell. An example of a gas-gap heat switch is shown in Figure 1.

2. Astro-H Flight Switch Design
The switches described here are an updated version of those developed for the engineering model of the adiabatic demagnetization refrigerator (ADR) created for the soft X-ray spectrometer (SXS) on the Astro-H mission [1, 2, 3]. These switches are the final flight design. Thus, they

are robust enough to survive the brutality of a rocket launch yet maintain the necessary on and off conductances to meet the requirements of a cooling system designed to hold a detector array at 0.050 K for more than 24 hours yet recycle within a one hour time frame. These last two requirements play a major role in the design of the heat switch.

2.1. Titanium Reentrant shell
The engineering model of the 3-stage ADR uses heat switches connected to the coldest two stages that integrate a composite material as the structural portion of the hermetic outer shell [2]. These shells are bonded into two copper flanges using epoxy. In that design, the hermeticity of the composite tube is provided by a thin foil of titanium 15V 3Sn 3Cr 3Al (typically shortened to Ti 15-3-3-3) bonded to the shell's interior surface. The composite shell, either T-300 carbon fiber or gamma-alumina, and the titanium foil, being only 0.05 mm thick, contribute less than 1 μW of heat load from 0.5 K to the 0.050 K stage of the ADR while in the off state. However, concerns over the foil-adhesion lifetime led to a design change for the flight heat switches.

It was decided that a metal shell brazed into two metal flanges is a more robust design, both structurally and hermetically. However, the thermal conductance of a metal tube that is thick enough to allow a pressure differential of up to one atmosphere demands the length of the tube be long. To fit into the pre-determined space allocated for the heat switches, the thermal length of the shell must fit into the spatial length of the composite-tube heat switches. Thus, for two of the four switches needed in the ADR, a reentrant design was developed that nested three tubes into the equivalent length of a single tube.

Even with the factor of three increase in the thermal length provided by the reentrant design, the metal chosen for the tubes must have the lowest thermal conductivity possible. Therefore, Ti 15-3-3-3 was used. This heavily alloyed titanium has one of the lowest thermal conductivities for a metal at temperatures below 10 K [4, 5]. This will be explored in section 3.

To make helium-leak-tight joints, we start with three concentric tubes. The middle tube is orbital welded to the largest tube at one end and the smallest tube at the other. Then, the free end of both the smallest and largest tubes are brazed into silver-plated 17-4 PH stainless steel flanges. Figure 1b shows a cross-sectional view of the switch with views of the orbital welds.

Two other heat switches are used in the ADR assembly. These connect a third ADR stage between the helium tank and a Joule-Thomson cryocooler [1]. It is not as critical to limit parasitic conduction through these switches because of the relatively warm temperatures involved. It is more important that they achieve relatively high on-state conductance since the cooling power of the stage is directly proportional to the rate at which heat can be absorbed from the helium tank and rejected to the cryocooler. Consequently, their design is simpler, consisting of a shorter, larger diameter body section containing the conductive fins, and a single cylindrical containment shell. Because the switch assembly is structurally supported in a cantilever fashion from the helium tank (see Figure 2) the switch mounted to the tank uses a 0.25 mm thick Ti 15-3-3-3 shell. The other switch uses a thinner 0.13 mm shell. In all other aspects, they are identical.

One concern regarding the reentrant design was the possibility of gas trapped in the dead space between the inner and middle shells. This gas has a small view factor and a high impedance path to the getter and may condense on the walls of the tube instead of the getter when the tubes become cold. If this occurs, then, when one end of the switch is warmed during a recycle of an ADR stage connected to it, there is the possibility that gas bound to these surfaces might desorb and begin to turn on the switch. This possibility has been discussed previously in the context of getters remote from the main body of a heat switch [2]. To date, there has been no evidence for this phenomenon in this design.
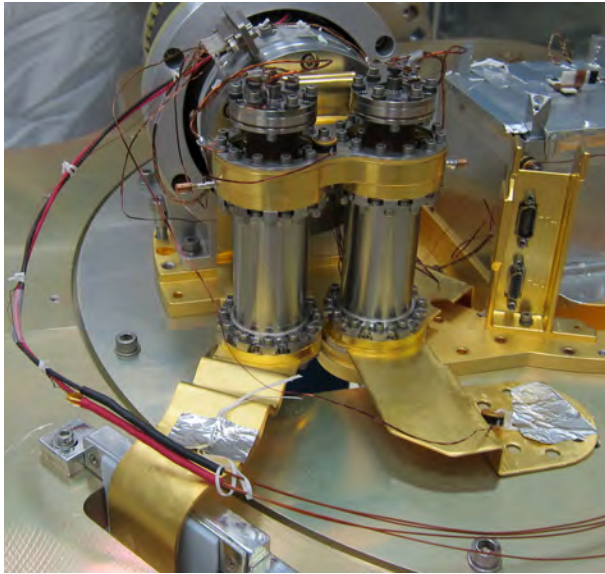
Figure 2. The heat switches associated with the third stage of the ADR. These are a larger diameter than those connected to the coldest stages of the ADR to enhance their on-state conductance. They also use a single-walled shell since the off-state conductance is not as critical here compared to the coldest two stages of the ADR. The switch on the right uses a shell wall thickness that is double the one on the left since the whole assembly is cantilevered from its base.

Figure 3. An indium seal is compressed between the flange brazed to the outer shell and the conducting fins inserted to the interior. The crenelated design of the flange allows the bolts that compress the indium seal to be taken out of the joint used to join the switch to other components. Since the heads of those bolts fit inside the machined opening in the flange and don't compress the indium seal, integrating or removing the switch from an assembly does not disturb the indium increasing its reliability.

2.2. Crenellated Flanges
Another improvement over the engineering model of the heat switches is a redesign of the flanges that are brazed onto the titanium tubes. By removing metal on the flanges we are able to produce a crenellated design that takes the screws that compress the indium seal between the interior conducting fins and the flanges out of the joint that attaches the switch to other components. Thus, integrating or removing the switch will not stress the indium and adds to the robustness of the seal. The crenellations may be seen in Figure 3.

3. Performance Data

3.1. Open-state conductance

When the gas, ^{3}He in this case, is sequestered in the getter, the end-to-end conductance of the heat switch is provided by the heat switch shell. Ti 15-3-3-3 has a conductivity lower than most metals used at cryogenic temperatures. This low conductivity is further enhanced once the material enters the superconducting state, about 3.9 K [5].

The thermal conductivity of Ti 15-3-3-3 in both the normal and superconducting states was fit to the following functions by Wikus *et al.* [5]:

$$\lambda = \begin{cases} \gamma T^\delta & T > T_c \\ \alpha T e^{-\beta T_c/T} & T < T_c \end{cases} \tag{1}$$

where α=0.043 W/m·K^2, β=0.27, T_c=3.89 K, δ=0.40, and $\gamma=\alpha\, T_c^{1-\delta} e^{-\beta}$=0.074 W/m·K^2.

Using (1) we may estimate the total conductance across the heat switch shell using the following:

$$\dot{Q} = \frac{A}{L} \int_{T_{\text{low}}}^{T_{\text{high}}} \lambda \, dT \tag{2}$$

where A and L are the cross-sectional area and length of the shell respectively, and T_{low} and T_{high} are the temperatures at each end of the heat switch. Thus we can estimate the expected contribution to the heat load on the Stage 1 salt pill due to the heat switch.

The three sections of the re-entrant containment shell for the heat switch have an average length and diameter of 6.35 cm and 2.06 cm, respectively, yielding an effective A/L of 0.0051 cm (the effective thermal length of the shell is 3 × 6.35 cm or 19.05 cm). This calculation omits the region of the shells where either an orbital weld or a braze joint is made. The thermal conductivity of the heat switch shells integrated over given temperature ranges are given in Table 1. These are compared in Table 2 with measurements of the total heat load on the ADR stage located at the cold end of the switch.

The difference between the total heat load and the calculated conductance through the heat switch is the heat load attributable to all other sources, all of which are thermally anchored to the helium tank at their warm end. In Figure 4 we plot the measured value for all heat flowing to the coldest ADR stage with the calculated contribution from the heat switch shell removed. In the same figure is shown the estimated contribution from the Kevlar suspension system for

Table 1. Estimated conductivity and heat flow across a heat switch made using a thin shell of Ti 15-3-3-3 in the open state. The shell dimensions are given in the text. This data is later used to determine heat flowing into the coldest stage of the ADR used in the Astro-H SXS cooler from sources other than the heat switch. Here, λ^* is the thermal conductivity integrated over the temperature range given in the table.

T_{low} (K)	T_{high} (K)	λ^* (mW/cm)	$\dot{Q}$ HS1 (μW)
0.050	0.5000	0.00285	0.01466
0.050	1.2000	0.08040	0.41347
0.050	1.4500	0.14500	0.74568
0.050	1.5000	0.16060	0.82590
0.050	1.5250	0.16800	0.86396
0.050	1.6250	0.20350	1.04650

Table 2. Heat load on the coldest stage of the Astro-H ADR for various helium tank temperatures. From here one can calculate the contribution from all sources other than heat switch connected to the coldest ADR stage.

Helium Tank Temperature (K)	Total Measured $\dot{Q}$ to Stage 1 of ADR (μW)	$\dot{Q}$ across HS1 shell from Table 1 (μW)	Calculated Non-HS1 $\dot{Q}$ to Stage 1 of ADR (μW)
1.200	1.2700	0.41347	0.85653
1.450	2.0310	0.74568	1.2853
1.500	2.2060	0.82590	1.3801
1.525	2.2900	0.86396	1.4260
1.625	2.6860	1.0465	1.6395

the salt pill of this stage using an aggregate A/L for the Kevlar of 0.01438 cm and a power-law description for the conductivity taken from Ventura *et al.* [6]. This is shown as a dotted line in the figure. Also plotted is the combination of the Kevlar contribution added to the function given for the estimated heat load from the detector assembly [7]. While the combination of the two contributions does not match our measured data precisely, the temperature dependence is remarkably similar and suggests that the calculated heat flow through the heat switch shell, which is in the superconducting state at these temperatures, is consistent with our measurements.

For the two switches associated with the third stage of the ADR, the A/L for both are 0.0469 and 0.0252 cm respectively (recall, one is thinner than the other by a factor of two). The two switches are in series between the tank at 1.2 K and the JT cooler at 4.5 K. When both are powered off, they have an equivalent A/L of 0.0164 cm. The integrated thermal conductance of Ti 15-3-3-3 over the temperature span is 2.77 mW/cm, giving an estimated conductance of 45 μW.

3.2. Closed-state conductance
When the switch is in the *on* or *closed* state, the heat flow path includes bolted joints, copper parts, and helium gas. These switches, when tested on their own, show a conductance near 1 K to be on the order of 100 mW/K. However, once integrated into a working ADR system, we often find this value drops to roughly half that value. The obvious mechanism for the lower-than-expected conductivity is the bolted joints that connect the switch to gold-plated copper thermal straps in the system. One may estimate the magnitude of conductance through a joint that contains two gold-plated copper pieces bolted together with a high force [8]. This estimation is consistent with the drop in conductivity measured in the full ADR system.

The time to activate the switch is less than one minute with a power of 0.300 mW applied to the getter. This short activation time is due to the getter design that combines a thermally isolated getter material with a low heat capacity. The design and performance of the getter are described elsewhere[2].

4. Qualification Programs
Since the crenellated flanges and the reentrant tubes are new for this design, it was determined a qualification program was necessary to prove flight worthiness.

For the flanges, we created heat switches with flight-like flanges and simulated the tubes and getters. These were then filled with ^{4}He. A total of six were anchored to the bottom flange of a vacuum vessel that was cooled to 77 K (using liquid nitrogen) a total of 69 times. A leak detector was tuned to sense ^{4}He and attached to the vacuum vessel. During the test, it was
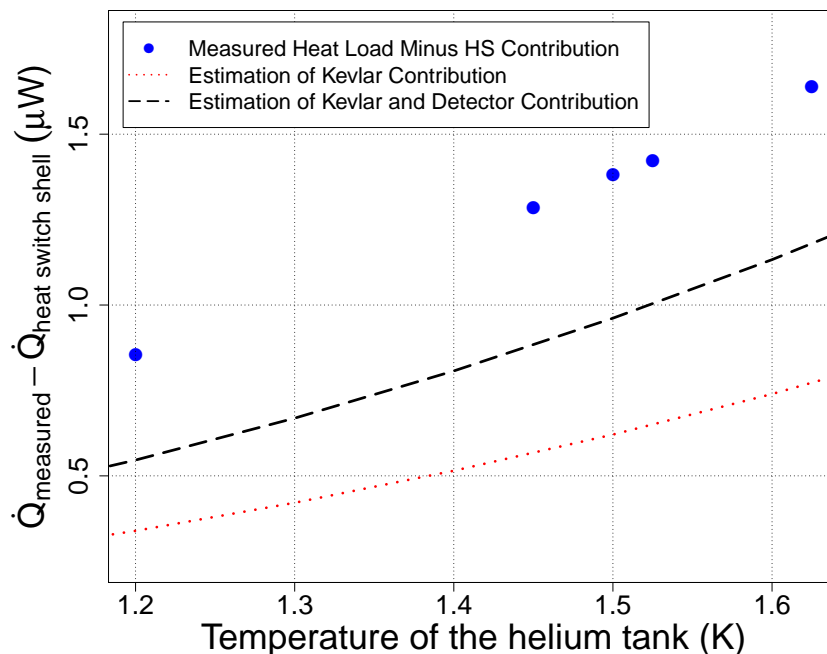
Figure 4. Heat flow to the coldest stage of the ADR when held at 0.050 K as a function of the helium tank temperature from all sources of heat except the heat switch shell. The dotted line is the estimated contribution of the Kevlar suspension system for the Stage 1 salt pill and the dashed line combines both the Kevlar contribution and the estimation of the heat load from the detector assembly. While there is still a discrepancy between the measured and calculated values, the temperature dependence is similar suggesting our calculation of the contribution from the heat switch shell is consistent with the data.

monitored to verify none of the indium seals failed at any point. The result was that none of the indium joints opened and therefore, the new flanges were qualified for use in the flight build. A photo of the bottom flange with six of the test pieces is shown in Figure 5.

Similarly, the flight tubes were welded into the reentrant shape then brazed into the flight flanges. This assembly was then put through a series of cool downs by submersing them into a bath of liquid nitrogen directly. The temperature drop was monitored so it occurred over one hour to prevent any thermal gradients and subsequent shock. After two cooling cycles, the tubes were leak checked to verify that simply cooling didn't open either the braze or weld joints. They were then pull tested to launch levels with margin after which they were leak tested again. All tubes passed this test, validating the design for spaceflight.

The original design of the heat switch shells used a carbon fiber composite tube for the hermetic outer shell. It was known that the vibration due to the launch of the satellite would compromise the structural integrity of these shells. Therefore the heat switches were surrounded by a titanium support structure from which the switches were suspended via Kevlar fibers. This structure and suspension is retained for the all-metal flight tubes. During cryogenic vibration testing it was verified that the structural loads imposed upon the heat switches during launch will be well below the allowable levels. This was the final test that qualified them for spaceflight use.

Figure 5. Model heat switches used to test the new flange design. This design allows the screws that mate the heat switch to other components in the system to not compress the indium seal (see also Figure 3). For the test, the switches are bolted to the end cap of a vacuum vessel and a thermometer is added to track the temperature of the cap. The assembly is then sealed to the vacuum vessel using an indium wire and cooled to 77 K slowly while measuring the presence of helium in the vessel interior.

5. Summary

We describe in detail the heat switches necessary for operation of the ADR built to fly on the Astro-H mission. These switches incorporate changes from the engineering model that enhance reliability. One of the major changes between the engineering model and final flight model designs is the substitution of a metal outer shell for a composite tube. This change trades robustness for an increased thermal conductivity when the switch is in the off state. At the time of this writing, the heat switches have been integrated into the flight model of the ADR. This, in turn, has been integrated into the SXS instrument and loaded into the flight dewar which was recently integrated to the spacecraft. Final testing is ongoing in anticipation of a launch in early 2016.

Acknowledgments

References

[1] Shirron P J, Kimball M O, James B L, Wegel D C, Martinez R M, Faulkner R L, Neubauer L and Sansebastian M 2012 *CRYOGENICS* **52** 165–171 ISSN 0011-2275
[2] Kimball M O and Shirron P J 2012 *Advances in Cryogenic Engineering, Vols 57A AND 57B* (*AIP Conference Proceedings* vol 1434) pp 853–858 ISBN 978-0-7354-1020-6 ISSN 0094-243X
[3] Mitsuda K *et al.* 2010 (*Proceedings of SPIE-The International Society for Optical Engineering* vol 7732) ISBN 978-0-8194-8222-8 ISSN 0277-786X
[4] Canavan E R and Tuttle J G 2006 (*AIP Conference Proceedings* vol 824) p 233
[5] Wikus P, Hertel S A, Leman S W, McCarthy K A and Ojeda S M 2011 *Cryogenics* **51** 41–44
[6] Ventura G, Barucci M, Gottardi E and Peroni I 2010 *Cryogenics* **40** 489–491
[7] Porter F S 2014 private communication NASA/GSFC
[8] Berman R and Mate C F 1958 *Nature* **182** 1661–1663 URL http://dx.doi.org/10.1038/1821661a0